

## DARK MATTER SUB-HALO COUNTS VIA STAR STREAM CROSSINGS

R. G. CARLBERG<sup>1</sup>

*Draft version June 3, 2019*

### ABSTRACT

Dark matter sub-halos create gaps in the thin stellar streams orbiting in the halos of galaxies. We evaluate the stream crossing integral with the guidance of simulations to find that the linear rate of gap creation,  $\mathcal{R}_U$  in a typical Cold Dark Matter (CDM) galactic halo at 100 kpc is  $\mathcal{R}_U \simeq 0.0022 \hat{M}_8^{-0.47} \text{ kpc}^{-1} \text{ Gyr}^{-1}$ , where  $\hat{M}_8 (\equiv \hat{M}/10^8 M_\odot)$  is the minimum mass halo that creates a visible gap. The relation can be recast entirely in terms of observables, as  $\mathcal{R}_U \simeq 0.023 w^{-0.82} \text{ kpc}^{-1} \text{ Gyr}^{-1}$ , for  $w$  in kpc, evaluated at 100 kpc. Examining the density variations in the NW stream of M31 we find that there are approximately  $12 \pm 2$  gaps over a length of about 200 kpc. For a 10 Gyr age the average rate at which gaps have been induced is  $0.006 \pm 50\% \text{ kpc}^{-1} \text{ Gyr}^{-1}$  in a 5 kpc wide stream. The Pal 5 stream has a gap creation rate of  $0.15 \pm 50\% \text{ kpc}^{-1} \text{ Gyr}^{-1}$  in a 0.11 kpc wide stream. The gap rate-width data are in good accord with the CDM predicted relation, about two orders of magnitude or more above the number of gaps that the visible sub-halos would create. The Pal 5 relation implies a total halo population of nearly  $10^5$  sub-halos above a minimum mass of  $2 \times 10^5 M_\odot$ .

*Subject headings:* dark matter; Local Group; galaxies: dwarf

### 1. INTRODUCTION

The dark matter halos in which galaxies are embedded are satisfactorily modeled as smooth quasi-isothermal spheroids, such as Hernquist (1990) or Navarro-Frenk-White (NFW, 1997) functions, as described in authoritative texts such as Binney & Merrifield (1998) and Binney & Tremaine (2008). Such mass models, with addition of the visible stars, gas and dust, can adequately account for most of the observed internal kinematics of galactic systems. On the other hand, N-body simulations of the formation of dark matter halos robustly predict that approaching 10% of the mass of any galactic dark halo should be in the form of sub-halos with numbers that rise steeply towards lower masses (Klypin et al. 1999; Moore et al. 1999; Springel et al. 2008; Diemand, Kuhlen & Madau 2007). The disk and bulge components of a galaxy will lead to sub-halo depletion in the central regions (D’Onghia et al. 2010). Although galaxies do contain visible dwarf galaxies embedded in sub-halos, the numbers are far short of the many thousands expected. Hence, it appears that either the predicted sub-halos are very dark, or, substantially not present.

An accurate census of the relatively low mass completely dark sub-halos remains a significant challenge. In principle the dark matter itself must have some cross-section for interaction with either itself or baryons, which could potentially give rise to annihilation radiation, but so far the non-detections have been useful to put upper limits on various candidate particles (Bergström & Hooper 2006; Essig et al. 2009). The gravitational effects of sub-halos, which are a high number density, hence becoming statistically smooth, small fractional mass, component of a galaxy, are fairly small. The sub-halos are potentially detectable through

micro-lensing of multiple-image background sources (Mao & Schneider 1998; Dalal & Kochanek 2002). The flux variations of multiple image lenses are definitely well explained with the presence of at least one moderately massive sub-halo, but with some concerns about intrinsic variability and differential extinction. Over a Hubble time sub-halos do lead to heating of some  $\sim 30 \text{ km s}^{-1}$  (Carlberg 2009). Such heating is not easily detectable in most of the visible components of a galaxy. However, the ongoing discovery of thin, low mass, stellar streams in galaxies opens up the possibility that the sub-halos can be detected through their gravitational effects on star streams. In particular, sub-halos that pass near or through a star stream create a gap in the stream (Ibata et al. 2002; Siegal-Gaskins & Valluri 2008; Yoon, Johnston & Hogg 2011; Carlberg et al. 2011; Helmi et al. 2011). Detecting gaps is easier than measuring stream kinematics, requiring only imaging data. The challenge of the image analysis is that the stars in any image are overwhelmingly in the foreground or background and the signal above the statistical noise at any point in the stream is often fairly low. Detections of gaps and lumps have been claimed with good statistical confidence for the Pal 5 stream (Odenkirchen et al. 2003; Grillmair & Dionatos 2006) and for the 100 kpc NW stream of M31 (Carlberg et al. 2011).

The purpose of this paper is to develop a basic analytic prediction of the rate at which sub-halos create visible gaps in star streams that can be applied to either simulations or observational data. In principle, the density of dark matter sub-halos (and other bound structures) in a galactic halo is simply measured with the number of times they cross a stellar stream to create visible gaps (Carlberg 2009; Yoon, Johnston & Hogg 2011). The rate at which gaps are created in a stream is the product of the density of sub-halos, the distance between sub-halo and stream which creates a gap, and the velocity at which sub-halos cross the stream. To use this sim-

<sup>1</sup>Department of Astronomy and Astrophysics, University of Toronto, Toronto, ON M5S 3H4, Canada carlberg@astro.utoronto.ca

ple measure of sub-halo density we need to allow for the mass spectrum of sub-halos and determine what range of velocities and impact parameters create visible gaps. In this paper we use a set of restricted n-body simulations to develop a gap creation rate formula. The rate predictions for CDM halos are compared to the available density field data on the 100 kpc loop of the NW stream of M31 (McConnachie et al. 2009) and the Pal 5 stream (Odenkirchen et al. 2003; Grillmair & Dionatos 2006).

## 2. THE GAP CREATION RATE

The rate at which gaps are created in a long thin stellar stream is the rate at which sub-halos of mass  $M$  with local volume density  $\mathcal{N}(r, M)$  cross the stream, integrated out to the maximum closest approach distance from the stream,  $b$ , which can create gaps. Full n-body simulations of the sub-halo content of halos find that the radial distribution and the mass function of sub-halos is separable into a radial dependence and a mass function,  $\mathcal{N}(r, M) = n(r)N(M)$  (Springel et al. 2008). The rate at which sub-halos cross the stream to create gaps is therefore,

$$\mathcal{R}_U(r) = \int_M \int_{v_\perp} \int_0^{b_{max}} n(r)N(M)v_\perp f(v_\perp)\pi db dv_\perp dM. \quad (1)$$

The factor of  $\pi$  arises from the consideration that in an isotropic velocity distribution for a circle of radius  $b$ , hence circumference  $2\pi b$ , half the stars will be headed inward.

An extensive set of restricted n-body simulations guides our approximate evaluation of the linear gap rate Equation 1 in a general context. Future studies will include full n-body simulations matched to observed systems. Here, the visible galaxy is approximated as a static potential with a small nuclear bulge and a Miyamoto-Nagai disk with the same parameters as Johnston (1998) used. To this we add an extended massive dark halo described with the NFW fit to the Springel et al. (2008) simulation of a Milky Way or M31 like galaxy. The stream is idealized as a circular ring of particles at 60 kpc, or 2 scale radii. At this large distance the halo dominates the enclosed mass. A ring of particles is initiated on tangential orbits at the local circular velocity,  $\sqrt{-\nabla\Phi \cdot r}$ . Most of the simulations are done with no initial random velocities but the particles are optionally given  $\sim 1\%$  epicyclic motions both in the orbital plane and perpendicular to it, which usefully obscures the small scale phase space details to make particle plots more comparable to observed streams. Only one sub-halo is sent towards the ring in each simulation. An individual sub-halo is adequately modeled as a Hernquist (1990) sphere with the mass-scale radius relation found in the Aquarius simulations, since for our purposes the exact details of the internal mass distribution are not important. The sub-halo motion is simply at a fixed velocity in a straight line, so it crosses the ring only once which avoids the complications of a sub-halo orbiting and having multiple ring crossings.

Figure 1 shows the result of a fairly massive satellite,  $10^9 M_\odot$ , passing over the ring at 0.6 and 6 kpc, top and bottom. As shown in the lower figure, flybys beyond the sub-halo scale radius do not lead to visible stream gaps.

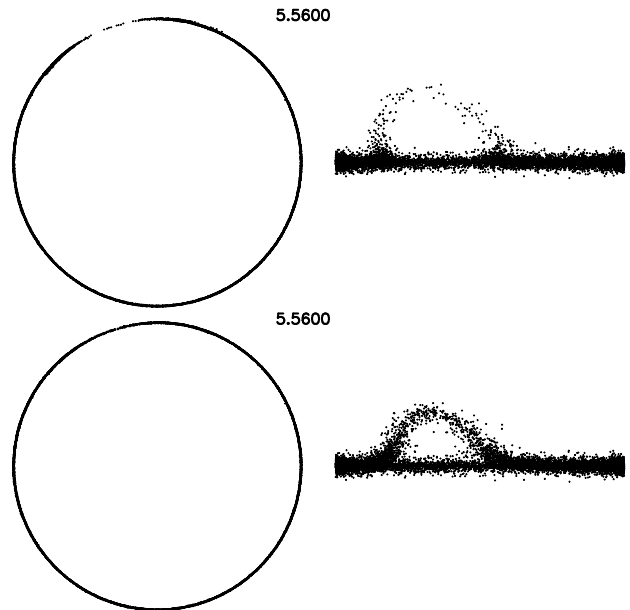


FIG. 1.— The top and side views, left and right respectively, of rings that have a sub-halo of mass  $10^9 M_\odot$ , scale radius 2.3 kpc, passing at a vertical height of 0.6 kpc (top) and 6 kpc (bottom). The top view is 132 kpc square, the side view is 6 kpc high. The ring has a velocity dispersion of about  $1 \text{ km s}^{-1}$ . The ring is shown at 5.56 Gyr, long after sub-halo has passed. Only the penetrating encounter leaves a readily visible gap.

Lower mass sub-halos create proportionally smaller vertical loops and gaps. To guide our analysis we measure various properties of the disturbed ring at intervals of about 1 Gyr starting about 2 Gyr after the sub-halo passes the ring. The vertical perturbations oscillate up and down in their orbit so we use the values from three separate epochs in our plots. The steps to evaluate the gap rate integral, Eq. 1, are first to determine the outcomes of sending single sub-halos past a ring, measuring the height, length and density dip in the gaps, from which we develop a model which can predict  $b_{max}$  in terms of sub-halo mass and encounter velocity, then we integrate over sub-halo velocities and the mass distribution, yielding the rate in terms of the minimum sub-halo mass,  $\hat{M}$ , that creates a visible gap. A related calculation gives the gap lengths in terms of sub-halo masses and can be used to create a relation between gap densities and stream width, both of which are measurable in imaging observations.

### 2.1. Sub-Halo Induced Stream Deflections

The impact approximation and the tidal approximation are the two general approaches used to describe the interaction of a satellite, such as a sub-halo, with a set of particles, the stars in the stream. The impact approximation is best suited to calculating deflections of individual stars from the rapid passage of a satellite and the tidal approximation is best suited to problems involving the differential gravitational field across a finite sized object. Both approaches are useful for calculating the gravitational heating of the perturbed objects and at their root both have the same underlying gravitational dynamics.

The impact approximation assumes that both a sub-

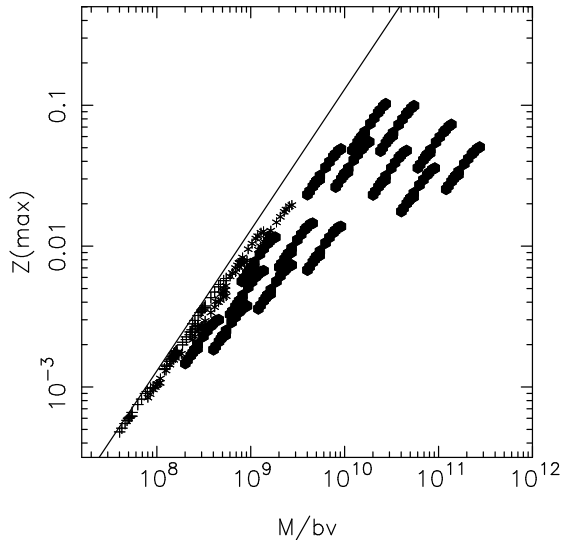


FIG. 2.— The maximum vertical height of a perturbation as a function of the impact strength parameter derived from the total sub-halo mass. The line is the prediction from the impact approximation. Each point represents a measurement in a simulation. Solid hexagons are used for points with  $b \leq 2R_s$ , asterisks for  $2R_s < b \leq 5R_s$  and plus signs for  $b > 5R_s$ , where  $R_s(M)$  is the scale radius of a sub-halo of mass  $M$ .

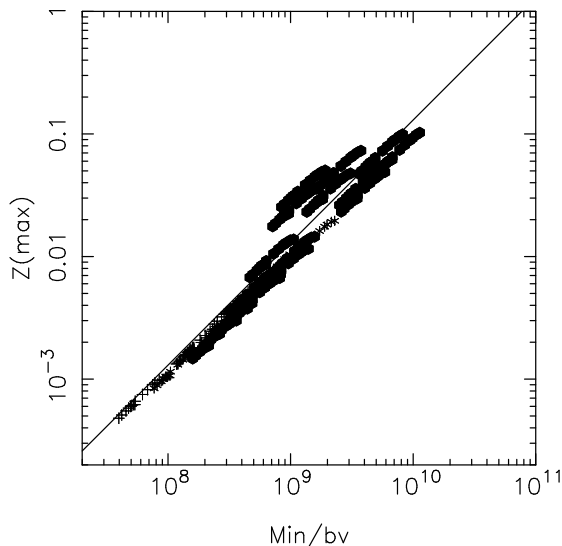


FIG. 3.— The maximum vertical height of a perturbation as a function of the impact strength parameter derived from the sub-halo mass within the distance of closest approach,  $M(b)$ . Some of the residual scatter is the result of the perturbed loop of stars oscillating up and down relative to the plane, so sometimes  $z_m$  is underestimated.

halo and a star stream orbit can be approximated as straight lines and sets aside the possibility that orbital resonances play a significant role. A sub-halo of mass  $M$  moving past a star at a relative velocity  $v$  with a distance of closest approach  $b$  will induce a velocity perpendicular to its direction of motion in the direction of closest approach of  $\delta v_{\perp} = 2GM/bv$ . If the orbit is approximately circular at radius  $r$  and  $\delta v_{\perp}$  is in the vertical direction, then conservation of angular momentum requires that the maximum orbital deviation out of the

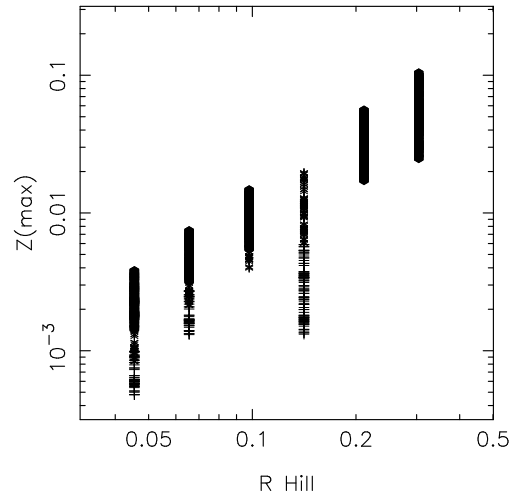


FIG. 4.— The maximum vertical height of a perturbation as a function of the tidal Hill Radius. The symbol meanings are the same as in Figure 2.

plane is  $z_m = r\delta v_{\perp}/v_c$ .

The impact approximation is readily tested with our simulations. In Figure 2 we plot the measured  $z_m$ , scaled to 30 kpc, against  $M/bv$ , where  $M$  is in solar masses and  $v$  scaled to  $210 \text{ km s}^{-1}$ . The predicted relation is shown as a straight line in Figures 2 and 3. Sub-halos with masses above  $3 \times 10^9 M_{\odot}$  are excluded from the plot since they usually catastrophically scatter the stream when they cross. Essentially all of the points fall below the predicted relation. The reason is simply that the sub-halos are far from being point-like masses. In Figure 3 we use the sub-halo mass inside the distance of closest approach,  $M(b)$ , as the mass and find generally good agreement. The velocities in this plot are the relative velocities between the sub-halo and the orbiting star particles. We conclude that the impact approximation with the mass interior to the impact parameter does a good job predicating the maximum height of a perturbation.

A key quantity in the tidal approximation is the Hill radius,  $r \sqrt[3]{M/(3M_t)}$ , which is the radius inside of which the gravitational field of the sub-halo, mass  $M$ , begins to dominate over the gravitational field of the total mass interior to the orbit of the stream,  $M_t$  produces the plot of Figure 4. Although the vertical perturbation and the Hill radius are strongly correlated there remains a large scatter that is strongly correlated with the scale radius of the satellite,  $b$ . Trying powers of  $b$  quickly shows that  $R_{Hill}b^{-1/3}$  removes some of the variation and even more if  $R_{Hill}$  is calculated from  $M(b)$ . This is hardly surprising since with the addition of  $v$  this becomes the impact approximation formula, multiplied by some constant factors. An alternative tidal quantity is the differential tidal field, which is proportional to  $M/b^3$ . A plot of  $z_m$  against  $M/b^3$  is mainly scatter. We conclude that the impact approximation is a better at predicting  $z_m$  than the tidal approximation.

We also need to consider the case of sub-halo moving vertically relative to the plane of the stellar stream's orbit. To a first approximation forces in the horizontal plane do not add to the angular momentum around the normal to the plane of the orbit, but do act to coherently

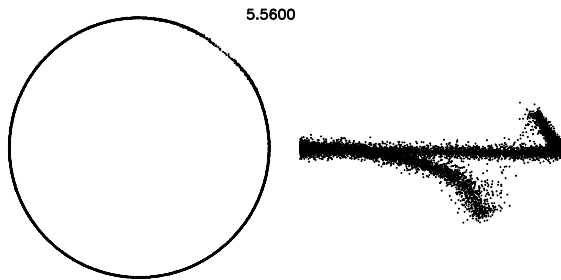


FIG. 5.— The same plot as Fig. 1 but for the sub-halo moving vertically, bottom to top, relative to the plane of the stream.

increase the epicyclic motion around the guiding center, but that makes little difference to the stream density. A sub-halo moving upward perpendicular to the orbital plane initially pulls the stream down and then up, which evolves into a paired set of peaks perpendicular to the orbital plane, as shown in Figure 5. The amplitude of the perturbation is again governed by the distance of closest approach so can use the same approximate analysis as used for a horizontally moving sub-halo. The one major difference in our analysis of a vertical sub-halo passage is that the amplitude of the perturbation is measured as the vertical distance from the positive peak to the negative peak, rather than the measurement of the absolute value of the offset from the initial orbital plane for a horizontal sub-halo passage. The resulting  $z_m$  shown in Figure 6 reasonably follows the same prediction as in Figure 3, although with more scatter and some systematic deviation. The density of particles in the gap is calculated half way between the two peaks. Figure 6, show the same basic behavior as for horizontal sub-halo motion, Figure 3. The important conclusion is that mean relations which describe the size of the perturbation and depth of gap for sub-halos moving either horizontally or perpendicular to the plane of the orbit are essentially the same. Interactions at other angles will be a superposition of these two responses which leads to an outcome with little sensitivity to the exact angle that a sub-halo passes through the plane of a star stream’s orbit.

### 2.1.1. Gap Parameters

We need to determine the maximum impact parameter that creates a visible gap. The density in the gap relative to the mean density in the ring as a function of  $b/R_s$  is shown in Figures 7 and 8, for horizontal and vertical sub-halo motions. For large impact parameter encounters the density in the loop pulled out of the ring is almost unchanged relative to the ring. That is, there is effectively no visible gap unless the sub-halo substantially penetrates the star stream. We will model this as a step function in the scale radius of a sub-halo, with gaps created for  $b \leq \alpha R_s(M)$  and no gaps for larger  $b$  values.

The length of a sub-halo induced gap as a function of the sub-halo parameters is needed to determine what gaps are large enough to be visible. We measure the gap length at 50% (the FWHM) of the maximum vertical height. The basis of a relation is visible in Figure 9 where we see that for substantially penetrating encounters,  $b/R_s < 1$ , that the ratio of the gap length to  $z_m$  is roughly a constant. The distribution has a logarithmic mean of  $w = 10^{1.52 \pm 0.13}$ , or  $w = 31z_m$ , with a scatter of

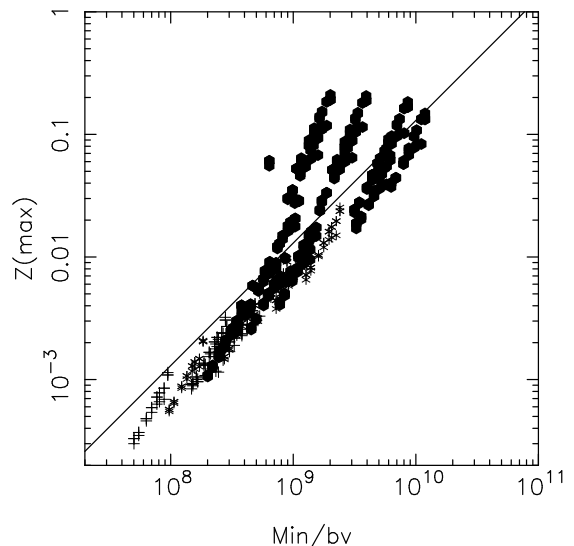


FIG. 6.— The same as Fig. 3 but for a sub-halo moving vertically.

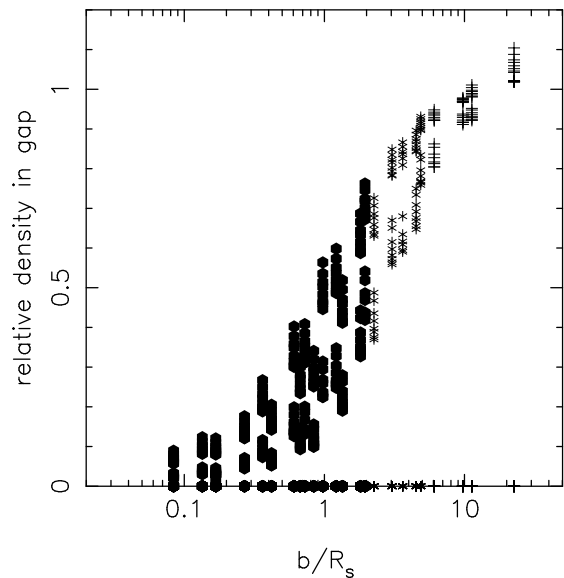


FIG. 7.— The linear density of particles in the plane of the ring as a function of the distance of closest approach normalized to the scale radius of the sub-halo. This plot is for a sub-halo moving horizontally above the plane of the star stream orbit.

38%. For vertical motions of sub-halos we measure the FWHM between the 50% points of the outermost parts of the upper and lower peaks, finding  $w = 10^{1.77 \pm 0.50}$ . This overlaps the horizontal relationship but has far more scatter and a somewhat larger mean. We will adopt the horizontal value in our calculations but note that there is significant variance in the  $w - z_m$  relationship.

### 2.1.2. The Characteristic Velocities

The rate at which sub-halos cross the stream depends only on  $v_{\perp}$ , which for an isotropic velocity dispersion normalized as  $\int f(v) dv = 1$  has a mean forward velocity of  $\int v f(v) dv = \sqrt{\frac{2}{\pi}} \sigma$ , which is approximately  $0.80\sigma$ . Note

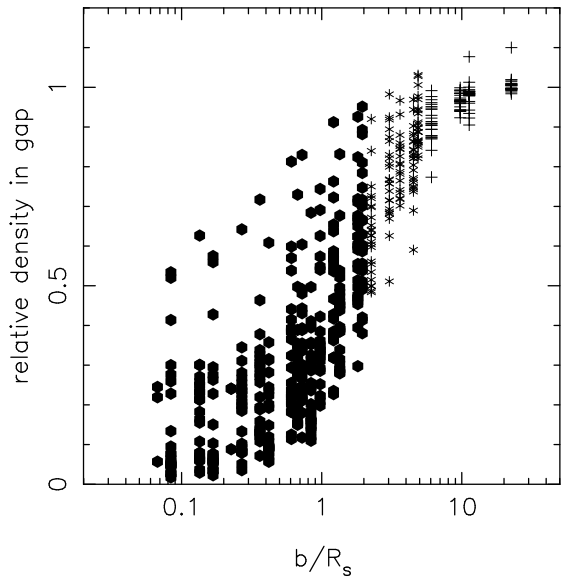


FIG. 8.— The same as Fig. 7, except for a sub-halo moving vertically.

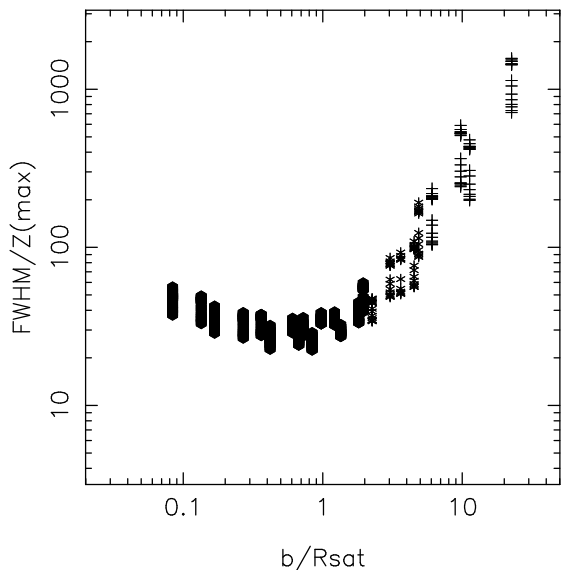


FIG. 9.— The ratio of the linear size at 50% of maximum height of the sub-halo induced “loop” to the vertical height as a function of the impact parameter in ratio to the scale radius of the sub-halo.

that the stream crossing velocity  $v_{\perp}$  does not include the mean motion of particles in a stream and is usually significantly smaller than the relative encounter velocity of a star and a sub-halo.

Star streams have a mean particle motion close to the circular velocity. Therefore the encounter speed between a sub-halo and a star in the stream, which is required for the impact approximation, will on the average be higher than the mean circular velocity. A consequence is that low velocity encounters of sub-halos with the stream are extremely improbable. Taking the mean encounter along the stream to be  $v_c$  and the velocity dispersion in the two axes perpendicular to the stream as  $\sigma$  the typical relative velocity is  $\sqrt{v_c^2 + 2\sigma^2}$ . Using  $\sigma \simeq v_c/1.8$  in the outer

part of a galactic halo then the typical sub-halo star relative encounter velocity is  $1.27v_c$ . The full triple velocity integral has the complication that there is a singularity at relative velocity of zero. Physically this would correspond to the velocity of the stream’s progenitor sub-halo. Inserting a very small “core” velocity of about one meter per second, we find that the mean encounter velocity is  $1.077v_c$ . Combining these factors we find that on the average,

$$z_m \simeq \frac{2GM_r}{1.08v_c^2 b}. \quad (2)$$

### 2.1.3. The Gap Creation Rate

We now have the elements to evaluate the gap creation rate, Eq. 1. The maximum impact parameter which creates a gap is  $b_{max} = \alpha R_s(M)$ , where our simulations find  $\alpha \sim 1$ . Evaluating the  $b$  and  $v_{\perp}$  integrals gives,

$$\mathcal{R}_{\cup}(r) = 0.80\pi\alpha\sigma n(r) \int_{M_{min}}^{M_{max}} N(M)R_s(M)dM. \quad (3)$$

The Aquarius simulations (Springel et al. 2008) find that  $R_s \simeq 0.83M_8^{0.43}$  kpc and that the mass distribution function is  $N(M)dM = 234M_8^{-1.9}dM_8$ , where  $M_8 = \hat{M}/10^8 M_{\odot}$ . The mass function gives the total number of sub-halos contained within the volume,  $V_{50}$ , that has a mean interior density 50 times the critical density which has a radius 433 kpc (Springel et al. 2008). Putting these pieces together we find,

$$\mathcal{R}_{\cup}(r) = 490\alpha\sigma V_{50}^{-1} \frac{n(r)}{n_0} \int_{\hat{M}_8}^{\infty} M_8^{-1.9} M_8^{0.43} dM_8, \quad (4)$$

where  $\hat{M}_8$  is the smallest mass mass halo that can create a visible gap. The mass integral is dominated by the smaller masses so we have set the upper mass limit to infinity. Evaluating the integral, choosing a local  $\sigma = 120 \text{ km s}^{-1}$  and converting to astronomical units, we find,

$$\mathcal{R}_{\cup}(r) \simeq 0.0022 \alpha \frac{n(r)/n_0}{6} \frac{\sigma}{120 \text{ km s}^{-1}} M_8^{-0.47} \text{ kpc}^{-1} \text{ Gyr}^{-1}, \quad (5)$$

where we have used the Springel et al. (2008) finding that the sub-halo density at 100 kpc is about 6 times the mean. The rate at which gaps are created increases with the minimum mass sub-halo that can create a noticeable gap, i.e.  $\mathcal{R}_{\cup} \propto \hat{M}^{-0.47}$ .

### 2.2. Gap Lengths

We can estimate typical gap length as a function of sub-halo mass, after integrating over the velocity distribution. The gap length-mass relation can either be used as a consistency test, or, taken a step further and be used to eliminate the unobservable minimum mass parameter from the rate equation in favor of a minimum gap length. Figure 9 guides our calculation. For  $b \leq R_s$  the logarithmically averaged value of  $l/z_m$  is  $31 \pm 38\%$ . Combining this average value, Equation 2 and setting  $b = R_s(M)$ , we find that the gap length is,

$$l \simeq 31r \frac{2GM(R_s)}{1.08R_s(M)v_c^2}. \quad (6)$$

Approximating a sub-halo density profile as a Hernquist profile we find that the mass inside the scale radius is

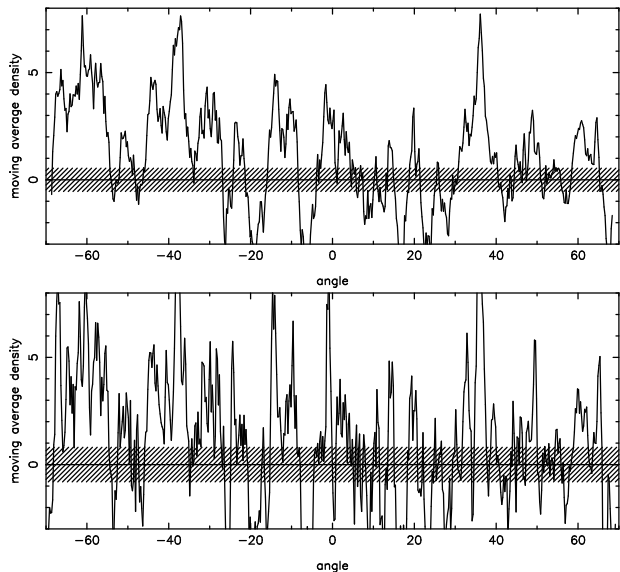


FIG. 10.— The linear density of stars  $\text{kpc}^{-2}$  in the M31 NW star stream with moving average of 5.5 kpc (top) and 2.5 kpc (bottom). The hatched areas are the  $\pm 1\sigma$  average error of the mean.

$M(R_s) = 1/4M$  (Hernquist 1990). Evaluating the numerical factors we find,

$$l \simeq \frac{16.8r}{100\text{kpc}} M_8^{0.57} \text{ kpc}. \quad (7)$$

The expected total number of sub-halos increases steeply with mass,  $N(M) \propto M^{-1.9}$ , so to with the minimum gap length,  $l$ , as  $N(l)dl \propto l^{-2.58}dl$ , at a given radius within a galaxy. If we could detect smaller gaps we would be sensitive to the rapidly increasing number of lower mass sub-halos.

The width of the stream and the minimum visible gap size are linked through orbital dynamics. The stream width is largely the result of stars emerging through the tidal Lagrangian points with low initial velocity dispersion. The epicyclic approximation describes the subsequent motion of the stars with small velocity dispersions around a larger mean motion. An individual star follows an elliptical motion around the center of motion with comparable amplitudes in direction of the motion and perpendicular to the motion, hence the stream width and the epicyclic motion along the stream is of nearly equal size. Provided that the phase angles of the motion are not significantly correlated, any induced gap narrower than the stream will be blurred out. Therefore, if we take the width of the stream as an estimate of the minimum gap size, we can relate the gap creation rate to the width of stream,

$$\mathcal{R}_\perp \sim 0.023\alpha \left( \frac{n(r)/n_0}{6} \right)^{1.75} \left( \frac{r}{100\text{kpc}} \right)^{0.82} w^{-0.82}, \quad (8)$$

for  $w$  in kpc. This relation recasts the gap rate in terms of an observable, assuming that the CDM halo substructure model gives the correct density of sub-halos. Equation 8 is a useful observational test of the CDM sub-halo prediction.

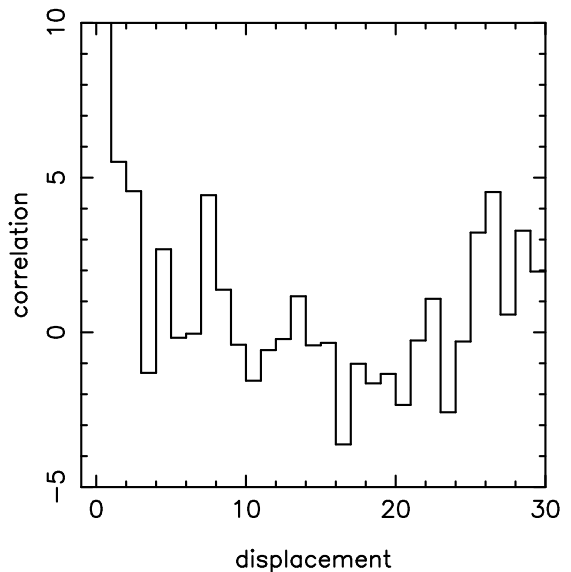


FIG. 11.— The cross-correlation of the density field measured in  $0.25^\circ$  bins. The correlation is positive for the first 4 or 5 points, indicating a scale of about 1 degree.

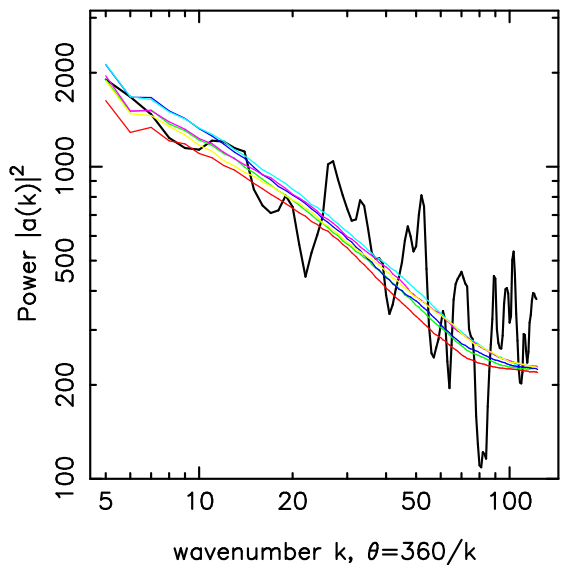


FIG. 12.— The power spectrum of the M31 NW stream compared to the mean power spectra of 96 simulations with 3, 10, 30, 100, 300 and 1000 sub-halos, from bottom to top. The simulation data has had white noise added to give  $\chi^2/\nu \simeq 1.5$ , for  $\nu = 128$ , similar to the M31 values.

### 3. GAPS IN THE NORTH-WEST STREAM OF M31

An accurate measurement of the density fluctuations and counting gaps in a star stream requires considerable statistical care because available observational data (McConnachie et al. 2009; Carlberg et al. 2011) has only a few stream stars per square kpc, and the mean density of the stream is only about 10-15% of the overall star density in the range of brightness and metallicities of interest. In Figure 10 we show the density field as a function of the angle around the star stream, with all quantities measured as reported in Carlberg et al. (2011). The plots are made with a moving average over 5 and 11 bins

of  $0.25^\circ$ , or roughly 2.5 and 5.5 kpc, respectively. We examine the statistics of the stream density to answer the question of how many gaps are present in the NW stream. First, to determine what scales in the stream appear to be physically correlated with plot the cross-correlation of the stream density minus the mean value with itself in Figure 11. We see that the stream densities are positively correlated over the first three bins of  $0.25^\circ$ , after which the fluctuations are essentially random. Therefore the smallest size scale we search for gaps in these data is about  $1^\circ$ , or, 2 kpc.

Figure 12 displays the power spectrum of the entire roughly half ellipse of the M31 NW stream density field, where the entire circle would have 256 bins. The resulting spectrum is smoothed with a running average over 11 frequencies. For comparison we plot the results of averaging together the power spectra of 96 simulations with the 3, 10, 30, 100, 300 and 1000 heaviest sub-halos. These power spectra have white noise added to obtain roughly the same  $\chi^2/\nu$  as in the observed stream. We can reproduce the main features of the power spectrum, however, the power spectrum is not a very sensitive indicator of the total number of sub-halos present. Gap counts are a better measure.

To count the gaps we need to have a good measure of the level of statistical fluctuations. The cross-correlation of the data with itself, at shifts beyond 5 bins, where there is no intrinsic signal, provides an accurate internal estimate the variance of the density field. The product of two normally distributed random variables is distributed like a modified Bessel function of the second kind and has a large kurtosis, 9, as compared to a normal distribution with a kurtosis of 3. However, the sum of many products (115 in our  $0.25^\circ$  sample) converges to a Gaussian distribution in accord with the central limit theorem. The kurtosis of  $n$  sums of products is  $3 + 6/n$  so declines fairly quickly with increasing  $n$ . The variance around the mean density of the data within the stream region, prior to background subtraction, is  $1.22$  (stars/kpc) $^2$ , and a comparable  $1.33$  in the background region. The background subtracted mean stream density has a variance of  $6.16$  (stars/kpc) $^2$ . The F ratio of the measured variance over the randomly expected variance is  $6.16/(1.22+1.33)=2.42$ , which has a random chance of occurrence of less than  $2 \times 10^{-5}$ . Larger bins give even higher significance that the measured stream density has variations well in excess of what is expected from random fluctuations. The conclusion and the levels of significance are in accord with the results presented in Carlberg et al. (2011) but use an independent line of argument which does not rely on an explicit calculation of shot noise statistics.

An estimate of the number of gaps is simply to count the number of times the density crosses down and up through some density threshold, requiring that the gap be at least the size of the smooth length. For a 5 point moving average at  $[-1\sigma, 0, +1\sigma]$  we find [11,11,15] gaps of mean length [7.1,6.9,15.1] bins, or, [1.8, 1.7, 3.8] kpc. Taking the stream length to be 200 kpc and using an age of 10 Gyr we find from the  $12 \pm 2$  gaps that the M31 NW stream has been subject to a mean gap creation rate of  $0.006 \pm 50\%$  gaps kpc $^{-1}$  Gyr $^{-1}$ . In principle the predicted rate also includes any sufficiently massive object,

but the detectable mass is well above the range for globular clusters and we do not expect molecular clouds along the large radius orbit of the NW stream.

The rate equation applied to the M31 NW stream requires a minimum sub-halo mass of  $\dot{M} = 1.2 \times 10^7 M_\odot$  and implies a total of 1700 sub-halos, which is a factor of 60 higher than 27 known dwarf galaxies of M31 (Richardson et al. 2011). The total number of sub-halos inferred from the data depends directly on the stream age,  $T$ , and the overlap parameter,  $\alpha$ , varying as  $\int n(M) dM \propto (\alpha T/10\text{Gyr})^{-1.8}$ . The mean gap length at  $+1\sigma$  is about 4 kpc and 2 kpc at  $-1\sigma$ . For the minimum halo mass of  $1.2 \times 10^7 M_\odot$  the mean minimum gap length is about 5 kpc (Carlberg et al. 2011). Hence, there is a good agreement between the predicted gap sizes and the observed lengths. Smaller gaps do not appear because the small residual velocity dispersion in the stream blurs them out.

The distribution of gap lengths should be in proportion to the mass spectrum as modified by the relation between the gap length and mass. That is the gap distribution should be a very steep function of the gap length,  $n(l) \propto l^{-2.6}$ . It is gratifying to note that the gap distribution is dominated by the smallest gaps, but the sample is too small with too little dynamic range to say much of statistical interest.

#### 4. THE PAL 5 STREAM

A narrow, hence low velocity dispersion, stream is predicted to have more visible gaps relative to wider stream at larger radius. The globular cluster Pal 5 has streams of 0.11 kpc width over 10 kpc (Odenkirchen et al. 2003; Grillmair & Dionatos 2006). Figure 3 of Grillmair & Dionatos (2006) at the  $3\sigma$  contour level indicates about 1 gap per degree over the  $22^\circ$  length. The relatively nearby and short stream Pal 5 stream may be dynamically younger than the Hubble age, although the cluster itself is very old. We assume a stream age of  $7 \pm 3$  Gyr to allow for the possibility that the Pal 5 cluster was disrupted well after its formation. Combining these estimates we derive  $0.15 \pm 50\%$  gaps kpc $^{-1}$  Gyr $^{-1}$ , which is best viewed as a lower limit since we have been unable to do the cross-correlation test applied the NW stream of M31 do determine a minimum scale.

The implied gap density in the Pal 5 stream is about 25 times higher than what we see in the M31 NW stream. The local density of sub-halos inside of about 20 kpc is a factor of 4 higher than at 100 kpc (Springel et al. 2008). The Pal 5 stream has a FWHM of about  $17' \pm 2'$ , which is about 0.11 kpc at a distance of 23 kpc (Harris 1996). Hence this stream is nearly a factor of 50 narrower than the M31 NW stream, which means that we expect to find many more gaps. The rate of gap creation in a stream at approximately 19 kpc from the galactic center (Harris 1996) is  $0.0088 M_\odot^{-0.47}$ , where the normalization has been increased by the factor of 4. The estimated Pal 5 gap density implies a minimum halo mass of  $0.25 \times 10^6 M_\odot$ . At this mass the minimum predicted gap size is 0.18 kpc, comparable to the 0.11 kpc width of the stream. The derived minimum mass implies a total of 57,000 sub-halos. A possible complication for the Pal 5 stream is that it will orbit through the plane of the galaxy where

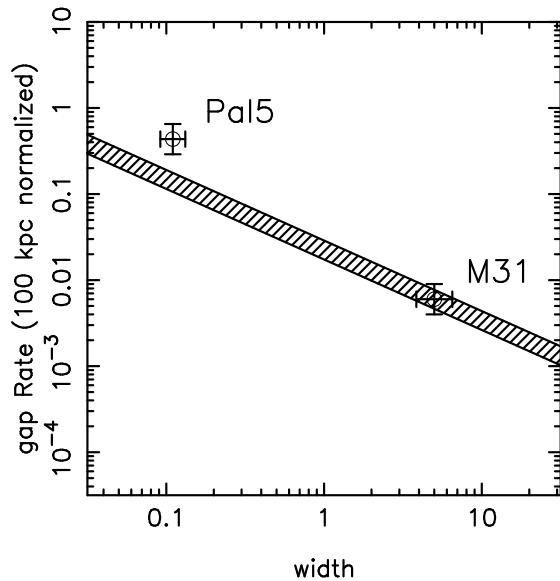


FIG. 13.— The estimated gap rate vs stream width relation for M31 NW, Pal 5 and the CDM halo prediction for  $\alpha = 1$ . A prediction using only the visible substructures within sub-halos would lower the predicted line roughly a factor of one hundred. The Pal 5 data have been normalized to 100 kpc. The width of the theoretical relation is evaluated from the dispersion in the length-height relation of Fig. 9.

it will be subject to disturbing effects of spiral arms and gas clouds that have masses and scale radii comparable to the dark matter sub-halos of interest.

## 5. DISCUSSION AND CONCLUSIONS

This paper lays a basis for understanding the rate at which visible gaps are created in long, thin, stellar streams. Restricted n-body experiments guide a calculation based on the impact approximation. The outcome is a prediction of the local rate at which gaps are induced in a stellar stream which effectively counts the number of sub-halos massive enough to produce visible gaps. Alternatively this can be recast as a relationship with the stream width, which gives a predicted relationship between observables that tests the CDM sub-halo prediction. The theory presented here could be further refined with full n-body simulations and of course more and better measurements of stream density profiles would be especially welcome. The results of this paper are largely encapsulated in Figure 13, which plots the measured and predicted gap rates against the widths of the streams. The Pal 5 data has been rescaled from a galactocentric distance of 19 kpc to 100 kpc. The agreement of the data and the CDM sub-halo prediction is remarkable. If one used the visible dwarf galaxies to predict the number of sub-halos the predicted density of gaps in these streams would be roughly a factor of 100 smaller, which would be in wild disagreement with the observation of virtually any gaps at all. The numerical consistency that we find is both an indirect and statistical test for the existence of the large predicted population of dark matter sub-halos.

This research is supported by NSERC and CIFAR.

## REFERENCES

- Bergström, L., & Hooper, D. 2006, *Phys. Rev. D*, 73, 063510  
 Binney, J., & Merrifield, M. 1998, *Galactic astronomy*, Princeton University Press, 1998  
 Binney, J., & Tremaine, S. 2008, *Galactic Dynamics: Second Edition*, Princeton University Press  
 Carlberg, R. G. 2009, *ApJ*, 705, L223  
 Carlberg, R. G., et al. 2011, *ApJ*, 731, 124  
 Dalal, N., & Kochanek, C. S. 2002, *ApJ*, 572, 25  
 Diemand J., Kuhlen M., Madau P., 2007, *ApJ*, 667, 859  
 D’Onghia, E., Springel, V., Hernquist, L., & Keres, D. 2010, *ApJ*, 709, 1138  
 Essig, R., Sehgal, N., & Strigari, L. E. 2009, *Phys. Rev. D*, 80, 023506  
 Grillmair, C. J., & Dionatos, O. 2006, *ApJ*, 641, L37  
 Harris, W.E. 1996, *AJ*, 112, 1487  
 Helmi, A., Cooper, A. P., White, S. D. M., Cole, S., Frenk, C. S., & Navarro, J. F. 2011, arXiv:1101.2544  
 Hernquist, L. 1990, *ApJ*, 356, 359  
 Ibata, R. A., Lewis, G. F., Irwin, M. J., & Quinn, T. 2002, *MNRAS*, 332, 915  
 Johnston, K. V. 1998, *ApJ*, 495, 297  
 Johnston, K. V., Spergel, D. N. & Haydn, C. 2002, *ApJ*, 570, 656  
 Klypin, A., Kravtsov, A. V., Valenzuela, O., & Prada, F. 1999, *ApJ*, 522, 82  
 Mao, S., & Schneider, P. 1998, *MNRAS*, 295, 587  
 McConnachie, A. W., et al. 2009, *Nature*, 461, 66  
 Moore B., Ghigna S., Governato F., et al., 1999a, *ApJL*, 524, L19  
 Navarro, J. F., Frenk, C. S., & White, S. D. M. 1997, *ApJ*, 490, 493  
 Odenkirchen, M., et al. 2003, *AJ*, 126, 2385  
 Richardson, J. C., et al. 2011, *ApJ*, 732, 76  
 Siegal-Gaskins, J. M., & Valluri, M. 2008, *ApJ*, 681, 40  
 Springel, V. et al. 2008, *MNRAS*, 391, 1685  
 Yoon, J. H., Johnston, K. V., & Hogg, D. W. 2010, *ApJ*, 731, 58

